Journal of Insect Physiology 85 (2016) 76–85

Contents lists available at ScienceDirect

Journal of Insect Physiology

journal homepage: www.elsevier.com/locate/jinsphys

Cold adaptation mechanisms in the ghost moth *Hepialus xiaojinensis*: Metabolic regulation and thermal compensation

Wei Zhu [a,b,1], Huan Zhang [a,1], Xuan Li [a], Qian Meng [a,b], Ruihao Shu [a,b], Menglong Wang [a], Guiling Zhou [a], Hongtuo Wang [a], Lin Miao [a], Jihong Zhang [a,*], Qilian Qin [a,*]

[a] State Key Laboratory of Integrated Management of Pest Insects and Rodents, Institute of Zoology, Chinese Academy of Sciences, Beijing 100101, China
[b] University of Chinese Academy of Sciences, Beijing 10049, China

ARTICLE INFO

Article history:
Received 6 August 2015
Received in revised form 5 November 2015
Accepted 10 November 2015
Available online 14 November 2015

Keywords:
Cold adaptation
Energy metabolism
Metabolic shift
Metabolomics
Mitochondrial cristae density
Thermal compensation
Hepialus xiaojinensis

ABSTRACT

Ghost moths (Lepidoptera: Hepialidae) are cold-adapted stenothermal species inhabiting alpine meadows on the Tibetan Plateau. They have an optimal developmental temperature of 12–16 °C but can maintain feeding and growth at 0 °C. Their survival strategies have received little attention, but these insects are a promising model for environmental adaptation. Here, biochemical adaptations and energy metabolism in response to cold were investigated in larvae of the ghost moth *Hepialus xiaojinensis*. Metabolic rate and respiratory quotient decreased dramatically with decreasing temperature (15–4 °C), suggesting that the energy metabolism of ghost moths, especially glycometabolism, was sensitive to cold. However, the metabolic rate at 4 °C increased with the duration of cold exposure, indicating thermal compensation to sustain energy budgets under cold conditions. Underlying regulation strategies were studied by analyzing metabolic differences between cold-acclimated (4 °C for 48 h) and control larvae (15 °C). In cold-acclimated larvae, the energy generating pathways of carbohydrates, instead of the overall consumption of carbohydrates, was compensated in the fat body by improving the transcription of related enzymes. The mobilization of lipids was also promoted, with higher diacylglycerol, monoacylglycerol and free fatty acid content in hemolymph. These results indicated that cold acclimation induced a reorganization on metabolic structure to prioritise energy metabolism. Within the aerobic process, flux throughout the tricarboxylic acid (TCA) cycle was encouraged in the fat body, and the activity of α-ketoglutarate dehydrogenase was the likely compensation target. Increased mitochondrial cristae density was observed in the midgut of cold-acclimated larvae. The thermal compensation strategies in this ghost moth span the entire process of energy metabolism, including degration of metabolic substrate, TCA cycle and oxidative phosphorylation, and from an energy budget perspective explains how ghost moths sustain physiological activity in cold environments.

1. Introduction

Ghost moths (Lepidoptera: Hepialidae) are obligate hosts of *Ophiocordyceps sinensis* (Berk.) and the fungal stroma and moth larvae form a very important traditional Chinese medicine called dongchongxiacao (Sung et al., 2007). Ghost moths belong to the earliest lepidopteran lineage and have a primitive appearance (Wiegmann et al., 2002). They are cold-adapted stenothermal animals distributed in alpine meadows on the Tibetan Plateau between altitudes of 3600–5200 m (Jin et al., 2010; Tu et al., 2011). They mainly inhabit the soil layer 5–20 cm below the surface, where temperatures fluctuate between −5 °C and 15 °C throughout the year (Wang et al., 2006). The optimal temperature for development of ghost moths is between 12 °C and 16 °C (Chen et al., 2002; Liu et al., 2007; Zhu et al., 2009), at which their life cycle is completed within one year instead of 3–5 years under natural conditions (Tu et al., 2011). Ghost moths maintain feeding activity and growth at relatively cold temperatures, from 0 °C to a few degrees above zero (Guo et al., 2008; Tu et al., 2011; Wang et al., 2006). This prominent adaptation to cold has received little attention, but revealing the underlying mechanism of this capability is necessary to better understand the principles of environmental adaptation in insects and potentially culturing this economically important species in the future.

In ectotherms, cold exposure depresses the rate of basic metabolic processes and reduces activity such as respiration, locomotion,

* Corresponding authors.
E-mail addresses: zhangjh@ioz.ac.cn (J. Zhang), qinql@ioz.ac.cn (Q. Qin).
[1] Authors contributed equally to this work.

http://dx.doi.org/10.1016/j.jinsphys.2015.11.008
0022-1910/

feeding and development, especially when temperatures approach 0 °C (Block, 1990; Lee, 2010). Among the physiological processes influenced by temperature, the reduction in metabolic rate may be the most crucial to the overall physiological status of organisms because it is the energy-producing process sustaining the ATP expenditure of other physiological processes. To maintain energy metabolism homeostasis at low temperatures, ectotherms may either enter into metabolic suppression or sustain activity using thermal compensation strategies (Guderley and St-Pierre, 2002). Metabolic suppression (e.g. diapause) is characterized by delayed development, reduced locomotion and minimal feeding (Schiesari and O'Connor, 2013; Tauber et al., 1986; Vinogradova, 2007) via a coordinated suppression of ATP production and consumption (Storey and Storey, 2004). Thermal compensation makes it possible to maintain energy-intensive activities like locomotion, feeding and development at low temperatures and allows better exploitation of the environment (Cossins and Bowler, 1987), which is presumed to be the case for cold-adapted ghost moth species. Thermal compensation is a regulation strategy amongst many cold-adapted ectothermic species, including lugworms, bivalves, crocodiles and fish (Glanville and Seebacher, 2006; Guderley and St-Pierre, 2002; Sommer and Pörtner, 2002; Tschischka et al., 2000). It is characterized by high metabolic capacity at low temperatures in naturally or artificially cold-acclimated individuals (Cossins and Bowler, 1987; Horwath and Duman, 1983). Thermal compensation is also found as part of seasonal cold adaptation in insects such as *Acheta domesticus* L. (Lachenicht et al., 2010), *Pyrrharctia isabella* (Layne-Jr et al., 1999), *Dendroides canadensis* and *Dendroides concolor* (Horwath and Duman, 1983) and plays a role in rapid environmental adaptation along latitudinal clines in insects (Addo-Bediako et al., 2002; Huey and Pascual, 2009). Though thermal compensation potentially explains environmental adaptation of insects across time and space, subsequent metabolic, physiological and compensation regulation strategies have been poorly studied.

Here, thermal compensation phenomenon in larvae of the ghost moth *Hepialus xiaojinensis* were confirmed at a physiological level. Considering that metabolites are the end products of cellular processes and that variation is expected to reflect the final regulatory effect of molecular signal transduction and explain physiological phenomena intuitively (Bundy et al., 2008; Nicholson and Lindon, 2008; Wishart, 2007), metabolomics based on gas chromatography-mass spectrometry (GC–MS) was chosen to initially explore system-wide metabolic adjustments at cold stress. Then, transcriptional, enzymatic and subcellular parameters were determined to supplement the metabolomic data. Our aim was to describe cold adaptation regulation mechanisms in this insect and identify potentially novel energy metabolism and thermal compensation strategies.

2. Materials and methods

2.1. Insect rearing and cold acclimation

H. xiaojinensis pupae were collected from Xiaojin, Sichuan, China, and the colony was maintained in a 15 °C cold room in Beijing. After molting to the 3rd instar, larvae were reared individually on carrots in 10 cm plastic dishes in the dark. The 8th instar larvae, with average weight of 0.584 ± 0.02 (mean ± SE), were randomly used for all experiments comparing the cold-acclimated and control (unacclimated) groups. The cold-acclimated group was treated at 4 °C for 48 h, and its respiration rate at 4 °C were measured at 24 and 48 h after cold acclimation respectively. The control group was maintained at 15 °C. Other ambient conditions were kept the same between the two groups. It must be mentioned that an acclimation course of 48 h was chosen for its obvious compensation effect on respiration at 4 °C. Besides, a short but effective acclimation course could avoid unexpected outcomes resulting from growth and be able to detect the adaptive adjustments at a transcriptional level, which may not last very long. After temperature regimes, the larvae of both groups were immediately used in subsequent experiments or material preparation.

2.2. Measurement of metabolic rate

We used a Sable Systems respirometry system (Las Vegas, USA) to measure metabolic rate (represented by the production rate of CO_2 and the consumption rate of O_2). The system included an SS-3 subsampler unit, MFC-2 Gas Mixers and Mass Flow Controller, RM8 Gas Flow Multiplexer, CA-10A CO_2 analyzer, FC-10A O_2 analyzer, ExpeData and UI-2 package. For each test, larvae were placed into a respirometry cuvette serially connected to the Sable System, and the cuvette was set in a thermostatic chamber with a designated temperature of 15 °C, 12 °C, 8 °C or 4 °C. After the system was stable, measurement was carried out under a closed-circuit model with a gas flow at 228–236 ml/min for 10 min. Variation in CO_2 and O_2 were recorded using a real-time curve graph.

Respiration data from the Sable System were processed using associated ExpeData software. The CO_2 production rate or the O_2 consumption rate was calculated using the following formula:

$$\text{Metabolic rate} = \frac{\text{Slope} \times \text{Pressure} \times \text{Volume}}{\text{Temperature} \times \text{weight} \times R \times 100000},$$

where, metabolic rate is the production rate of CO_2 or the consumption rate of O_2, mol/s/g; slope is the curve slope of CO_2 production or O_2 consumption, read from ExpeData; pressure is the air pressure in the closed-circuit system, 101.9 kPa; volume is the volume of the closed-circuit system, 140 ml; temperature is the temperature of the closed-circuit system, K; and R is the ideal gas constant.

The Q_{10} coefficient of CO_2 production rate or O_2 consumption rate was calculated using the following formula:

$$Q_{10} = \left(\frac{R_2}{R_1}\right)^{\left(\frac{10}{T_2 - T_1}\right)},$$

where, Q_{10} is the factor by which the reaction rate increases when the temperature is raised by ten degrees; T_1 and T_2 are temperatures (K or °C); R_1 is the measured metabolic rate at temperature T_1 (where $T_1 < T_2$); and R_2 is the measured metabolic rate at T_2 (where $T_2 > T_1$).

2.3. Insect dissection and preparation of material

For each larva, hemolymph (30–60 μl) was collected through incisions made on the prolegs (Oda et al., 1997) and stored at −100 °C. Then, midgut and fat body were dissected from the abdomen and placed into separate Eppendorf tubes. After washing in Ringer's, tissues were stored at −100 °C.

2.4. Thin-layer chromatography (TLC) for total lipids in hemolymph

The method followed the extraction of total lipids by Bligh and Dyer (1959) with appropriate scaling in volume. In brief, 15 μl of hemolymph was mixed with 25 μl Mili-Q water, 50 μl chloroform and 100 μl methanol and pipetted repeatedly for 2 min. After a centrifuging procedure at 12,000*g* for 10 min the supernatant was transferred into a clean tube with 50 μl chloroform and 50 μl Milli-Q water, followed by 15 s of vortex. After being centrifuged at 10,000*g* for 10 min, the chloroform phase was collected with a syringe, and then dried in a vacuum drier. After being dissolved in 30 μl 2:1 chloroform:methanol, the total lipid sample was ready to analyze on the silica gel chromatography plate

(GF254 100*100, AR). The parameters of TLC were set according to Bao and Zhang (2013). After the development with hexane:diethylether:acetic acid (45:25:1, v/v), the plate was dried by an air blower and fully sprayed with 10% phosphomolybdic acid in ethanol. After coloration at 105 °C in an oven, the plate was saturated by ammonia to eliminate the background. The image of the plate was captured with the Gel Logic 200 Imaging System (Kodak). Dipalmitin (AR) was used as a chemical standard to identify dots of diacylglycerols (DAGs) in hemolymph samples.

2.5. Metabolic fingerprinting

2.5.1. Sample preparation

Samples were prepared for metabolic fingerprinting using the methods described by Pasikanti et al. (2008) with some modification. For hemolymph samples, 10 μl of hemolymph was sampled and extracted with 80 μl methanol plus 5 μl of 10 mg/ml heptadecanoic acid in methanol (internal standard, TCI) at 50 °C for 30 min. After centrifugation at 12,000*g* for 15 min (4 °C), the supernatant was transferred into a clean tube. For fat body samples, approximately 30 mg wet tissue was sampled and extracted with 80 μl methanol plus 10 μl internal standard (mentioned above) and 100 μl chloroform:methanol:water (2:5:2, v/v), successively. Each extraction step lasted 30 min at 50 °C, followed by centrifugation at 16,000*g* for 15 min at 4 °C. The supernatants were collected and merged. The supernatants from both the fat body and hemolymph were vacuum-dried at 40 °C, then oximated with 40 μl methoxyamine hydrochloride (20 mg/ml in pyridine, J&K) at 37 °C overnight. Then 40 μl N-methyl-N-trifluoroacetamide (MSTFA, SIGMA) was added to silylate the metabolites at 37 °C for 30 min. After derivatization was finished, 70 μl hexane (HPLC grade) was added and the samples were centrifuged at 12,000*g* for 15 min at room temperature. The supernatant was then ready for analysis.

2.5.2. Chromatographic analysis

The parameters of the gas chromatograph and mass detectors were set following Michaud et al. (2008) and modified according to our pre-experiments. Analyses were performed on an Agilent 6890N-5973N (Agilent Technologies). The following parameters were chosen: helium as the carrier gas; WCOT capillary GC column (60 m, ID 0.25 mm, film 0.25 μm, Agilent Technologies); 1 μl injection volume and splitless model; temperature of injectors, 250 °C; initial temperature of oven held stable at 90 °C for 1 min, followed by a 5 °C min^{-1} increase to 175 °C, then a 3 °C min^{-1} increase to 270 °C and a 5 °C min^{-1} increase to 310 °C, and finally stable for 12 min; and full-scan mode for mass spectrometer.

2.5.3. Identification and quantification of metabolites

Metabolites were identified following the guidelines of the metabolomics standards initiative (Sumner et al., 2007). In conclusion, the metabolites were confirmed by matching the mass spectra to reference spectra from the NIST08 library and overlaying the chromatographs with authentic standards. For metabolites confirmed exclusively through the mass spectrum comparison, a much stricter threshold (match value $\geqslant$ 750, reverse math value $\geqslant$ 800, and a probability $\geqslant$ 60) was set to ensure more reliable outcomes (Table S1).

The GAVIN package (based on Matlab) was used for area integration of the characteristic ion peak of each identified metabolite across samples (Behrends et al., 2011). The outcome of GAVIN was a quantitative area table (matrix of samples against metabolites). The area of internal standard (heptadecanoic acid) and weight of material (for fat body samples) were used for normalization of data, with the following equations:

$$A_N = A_O/(A_{IS}/A_{AIS}) \text{ for hemolymph samples,}$$

$$A_N = A_O/((A_{IS}/A_{AIS}) \times (W/W_A)) \text{for fat body samples,}$$

where, A_N = normalized area; A_O = original area; A_{IS} = area of internal standard; A_{AIS} = average area of internal standard across samples; W = weight of tissues; and W_A = average weight of tissues across samples.

2.6. Total fatty acid analysis of fat body

Extraction and methylation of fatty acids followed the methods of Kang and Wang (2005) with some modification. Homogenized samples of the fat body were placed in glass methylation tubes. Then, 1 ml of hexane (HPLC grade) and 1 ml of 14% BF3/MeOH reagent were added to each tube and mixed sufficiently. The mixture was heated at 100 °C for 1 h, followed by cooling to room temperature. After the addition of 1 ml water, the sample was centrifuged for 1 min and methyl esters were extracted into the hexane phase. The hexane phase was then removed and concentrated under nitrogen.

Fatty acid methyl esters were analyzed using a gas chromatograph equipped with mass detectors (Agilent 7890-5975). The parameters were chosen according to Mustonen et al. (2007). Briefly, the column and reaction conditions were as follows: DB-wax capillary column (30 m, ID 0.25 mm, film 0.25 μm, J&W Scientific, Folsom, CA, USA); 2 μl injection volume and 1:20 split ratio; temperature of injectors, 250 °C; initial temperature of the oven stable at 180 °C for 8 min, followed by a 3 °C min^{-1} increase to 210 °C and finally held stable for 25 min; and flow rate of the carrier gas, 1.0 ml min^{-1}. Peak identities were determined by overlaying the Total Ion Chromatographs with those of fatty acid mixture standards (SUPELCO, purchased from ANPEL). Matching mass spectra from the NIST08 database were taken for further verification. The integration of the area of individual peaks was performed using a manual model based on Agilent Chemstation, and the content was represented as the percentage of the total area.

2.7. Determination of enzyme activity

Fat body tissues were put into a 1.5 ml Eppendorf tube with 500 μl mitochondria lysate (20 mM Tris, 2 mM EGTA, 2 mM EDTA, 1% Triton X-100, pH 7.5). After adding 5 μl 100 mM PMSF, tissues were pipetted repeatedly and homogenized by a tissue grinder. Tubes were kept in an ice-bath for 100 min and shaken for 30 s on a vortex (QL-901) every 20 min. After centrifugation at 12,000*g* for 15 min (4 °C), supernates were collected as crude enzyme solutions. After determination of the protein concentration by Coomassie Brilliant Blue G250, all samples were diluted to the same protein concentration. The reaction system for determination of isocitrate dehydrogenase (IDH) included 16 μl diluted enzyme sample and 100 μl mixture (0.33 mM EDTA, 0.1 mM DTT, 33 mM Tris, 1.4 mM $MgSO_4$, 0.5 mM $NADP^+$, 7.5 mM isocitric acid trisodium salt hydrate). The optical density (OD) value at 340 nm was recorded every 10 s for a total of 1 min at room temperature. The IDH activity was defined as the increment of OD value per minute per milligram protein (OD/min/mg, at room temperature). The activity of succinate dehydrogenase (SDH) was measured by a SDH Assay Kit (Nanjing Jiancheng Bioengineering Institute, China) according to the manufacturer's instructions. The dehydrogenation of succinate was coupled with the reduction of 2,6-DPIP, and resulted in reduced absorption at 600 nm. The OD value at 600 nm was recorded every 10 s for a total of 1 min at room temperature. The enzyme activity was defined as the decrement of OD value per minute per milligram protein (OD/min/mg, at room temperature).

2.8. Real-Time PCR transcript quantification

Total RNAs from fat bodies were isolated using TRIzol reagent (Invitrogen, CA, USA). The reverse transcription procedure followed the protocol of SuperRT cDNA Kit (CWBIO). The reaction system of real-time PCR was constructed with the UltraSYBR Mixture (with ROX) (CWBIO), and the PCR was performed on Mx3000P (Stratagene, USA) with a temperature program as follows: 95 °C for 10 min; followed by 40 cycles of 95 °C for 15 s, 60 °C for 60 s; then a final melting cycle for 95 °C for 60 s, 55 °C for 30 s, 95 °C for 30 s. The sequences of primers and PCR products are detailed in Table S2. Sequences of referred genes were obtained by querying our RNA-seq database (unpublished data) of *H. xiaojinensis* larvae with known functional counterparts of other insect species.

2.9. Transmission electron microscope

After washing with PBS (0.1 M, pH 7.2), midguts were fixed in 1 ml 2.5% glutaraldehyde in PBS for 24 h at 4 °C. Then, the glutaraldehyde solution was removed and specimens washed with PBS repeatedly (7 min * 5). Similarly, specimens were post-fixed in 1% osmium tetroxide for 2 h at 4 °C and washed with PBS repeatedly (7 min * 5). Then, specimens were dehydrated through a graded (50%, 70%, 85%, 95%, 100%, 100%, 100%, 100%) ethanol–water series, each change taking 15 min. The specimens were embedded sequentially as follows: incubated in acetone:epoxy resin (2:1, v/v) for 1 h at 37 °C; incubated in acetone:epoxy resin (1:1, v/v) for 1 h at 37 °C; incubated in epoxy resin at 37 °C over night. After removing the epoxy resin, the specimens were further incubated for 24 h at 45 °C and 65 °C, successively. After cut into thin sections and stained with phosphotungstic acid, the specimens were examined with a JEM-1230 transmission electron microscope.

2.10. Statistical analysis

Variation in metabolic rates at different temperatures in unacclimated larvae was analyzed using one way ANOVA, and Student Newman Keuls post hoc tests were applied to identify the differences between temperatures. The production rate of CO_2 was $\log_2$ transformed to meet equal variance assumptions. The effect of cold acclimation on metabolic rate ($\log_2$ transformed to meet equal variance assumptions) and respiratory quotient (RQ, the ratio between CO_2 production and O_2 consumption) was analyzed using one way ANOVA and Student Newman Keuls post hoc tests. As the respiration data after cold acclimation at 24 and 48 h was collected from the same group of larvae, paired sample *T* test was also applied to identify the differences between these two groups. Analyses of other differences between groups were carried out using independent sample *T* tests. All statistical analyses were run using IBM SPSS v21 (SPSS Inc., Chicago, USA). Graphs were created using Graphpad prism 5 or ggplot2, an R package (R Core Team, 2014; Wickham, 2009).

3. Results and discussion

3.1. Metabolic rate and thermal compensation

The CO_2 production rate and O_2 consumption rate of control animals fluctuated between 3 and 4 nmol/g/s at their optimum

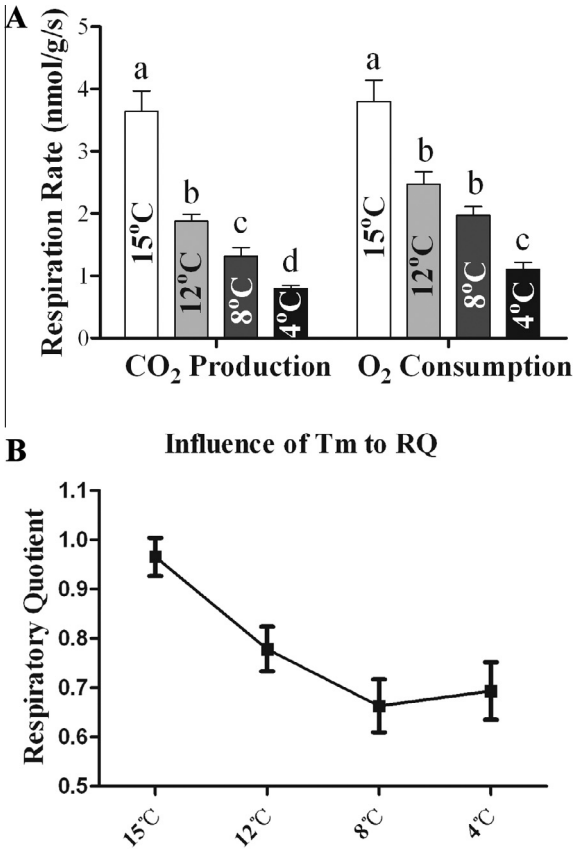

Fig. 1. The metabolic rate of un-acclimated *H. xiaojinensis* larvae. (A). Rates of CO_2 production and O_2 consumption with decreasing ambient temperature. Each column represents the mean ± SE of eight samples. Different letters indicate significant differences between values ($p < 0.05$), as shown by the Student Newman Keuls post hoc test after one way ANOVA. (B). Variation in respiratory quotient with decreasing temperature ($n = 8$, mean ± SE).

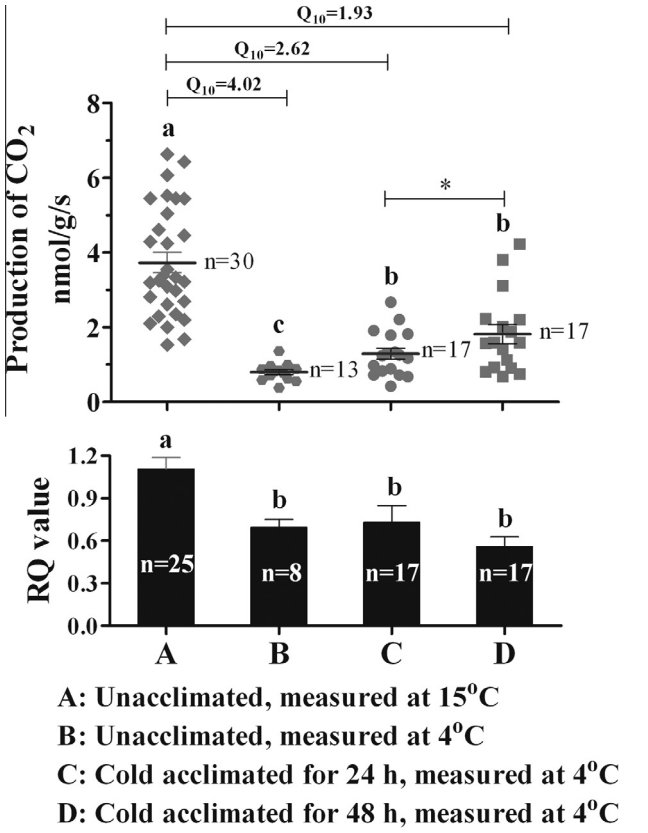

Fig. 2. The effects of cold acclimation on respiration. Values are mean ± SE. Different letters indicate significant differences between values ($p < 0.05$), as shown by the Student Newman Keuls post hoc test after one way ANOVA. Values of C and D groups were measured on the same larvae at 24 and 48 h after cold acclimation, respectively, and the asterisk indicates significant pairwise differences between these two groups at $p < 0.05$ (paired sample *T* test).

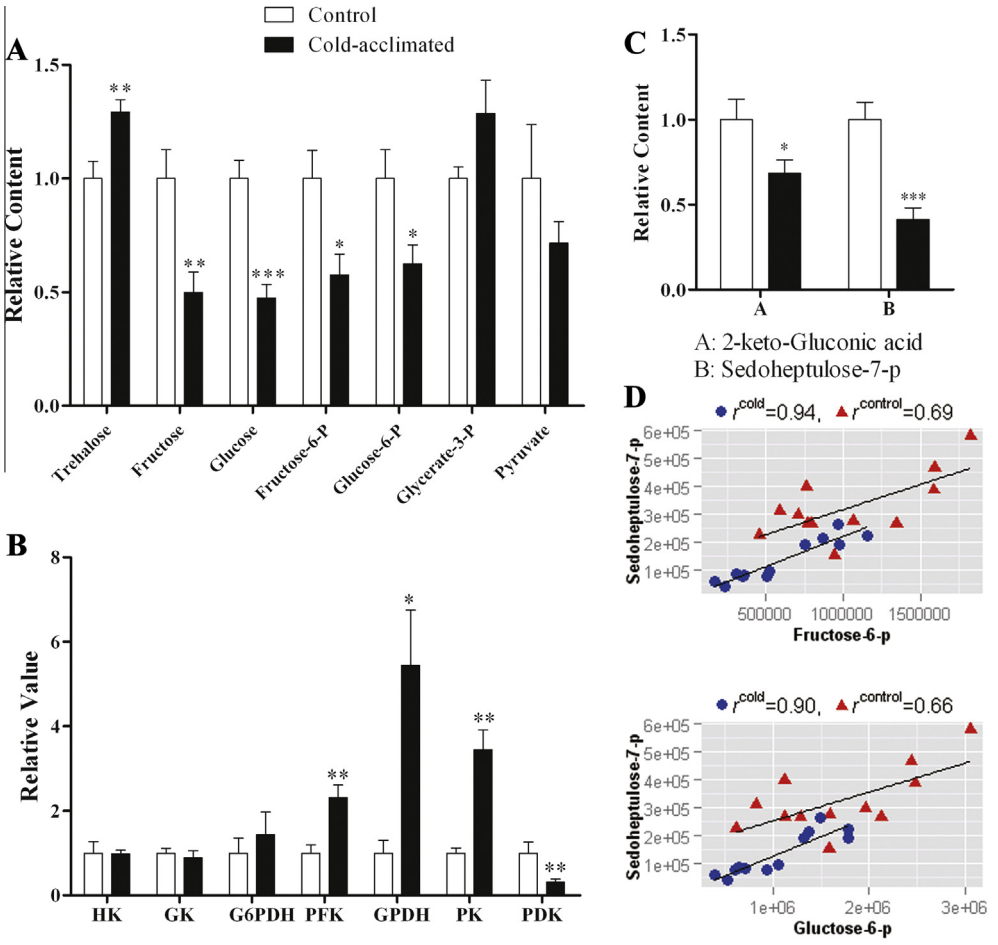

Fig. 3. Glycometabolism in cold-acclimated *H. xiaojinensis* larvae (white columns: control group; black columns: cold-acclimated group). (A). Variation of metabolites of glycolysis in fat body ($n = 12$). (B). Transcription level of enzymes in fat body by real-time PCR. HK: hexokinase ($n = 5$); GK: glucokinase ($n = 5$); PFK: phosphofructokinase ($n = 5$); GPDH: glyceraldehyde phosphate dehydrogenase ($n = 3$); PK: pyruvate kinase ($n = 3$); PDK: pyruvate dehydrogenase kinase ($n = 5$). (C). Variation of intermediates in pentose phosphate pathway ($n = 12$). (D). Linear correlation between metabolites. Each column represents a mean ± SE, ***: $p < 0.001$, **: $p < 0.01$, *: $p < 0.05$.

temperature of 15 °C. With decreasing ambient temperature, both of these declined (CO_2: $F_{3,28} = 47.65$, $p < 0.001$; O_2: $F_{3,28} = 47.65$, $p < 0.001$) and suggests that the respiration system of *H. xiaojinensis* larvae is sensitive to cold (Fig. 1A). The respiratory quotient (*RQ*, the ratio between CO_2 production and O_2 consumption) of *H. xiaojinensis* larvae reduced from 0.97 ± 0.10 (mean ± sd) at 15 °C to 0.69 ± 0.15 (mean ± sd) at 4 °C (Fig. 1B). Theoretically, *RQ* values of 1.0 and 0.7 indicate carbohydrates and lipids based energy metabolism, respectively. Though RQ values may not be used to estimate the composition of metabolic fuel in practice, its decreasing trend suggests that the devotion of carbohydrates to energy metabolism declines at sudden low temperatures, which may result from the susceptibility of glycometabolism pathways to temperature.

The production rate of CO_2 gradually increased with duration of exposure at 4 °C ($F_{3,73} = 31.16$, $p < 0.001$) with average Q_{10} values falling from 4.02 to 1.93 after acclimation at 48 h (Fig. 2). The metabolic rate after acclimation at 48 h was higher than that at 24 h ($p < 0.05$, paired sample *T* test). These results suggest that thermal compensation strategies have a role in cold adaptation in *H. xiaojinensis* larvae. There are two possible ways ghost moths can sustain sufficient energy production under fluctuating temperatures in their natural, cold habitat: cold-insensitive metabolic systems or energy metabolism thermal compensation. Our metabolic rate data rule out the former and support the latter. Moreover, cold acclimation did not increase the RQ value at 4 °C, suggesting that energy metabolism based on carbohydrates and lipids were compensated synchronously, and that lipids replaced carbohydrates as major metabolic substrate at cold condition.

3.2. Regulation of metabolic structure

3.2.1. Carbohydrate metabolism

Compared to the control group, cold-acclimated larvae had a higher concentration of trehalose, and lower concentrations of glucose, fructose, glucose-6-p and fructose-6-p in their fat body (Fig. 3A). Given that trehalose is a carbohydrate reserve in insects and that glucose, fructose, glucose-6-p and fructose-6-p are obligatory intermediates in the utilization of carbohydrates, the opposite variation trends might imply that the overall consumption of carbohydrate is dramatically depressed at 4 °C, even after acclimation for 48 h. This was supported by variation of those less abundant intermediates and disaccharides in fat body and hemolymph, respectively (Fig. S1).

To explore potential thermal compensation strategies for the utilization of carbohydrates in the fat body, the transcriptional levels of several enzymes were measured using real-time PCR (Fig. 3B). Accordingly, the transcription of hexokinase and glucokinase remained unchanged. In agreement with metabolomics, this suggests that the overall utilization of carbohydrates was not compensated. The transcription of glucose-6-phosphate dehydrogenase (G6PDH), the crucial enzyme controlling flux throughout the pentose phosphate pathway, was not significantly increased, with downstream metabolites detected in our study (2-keto-gluconic

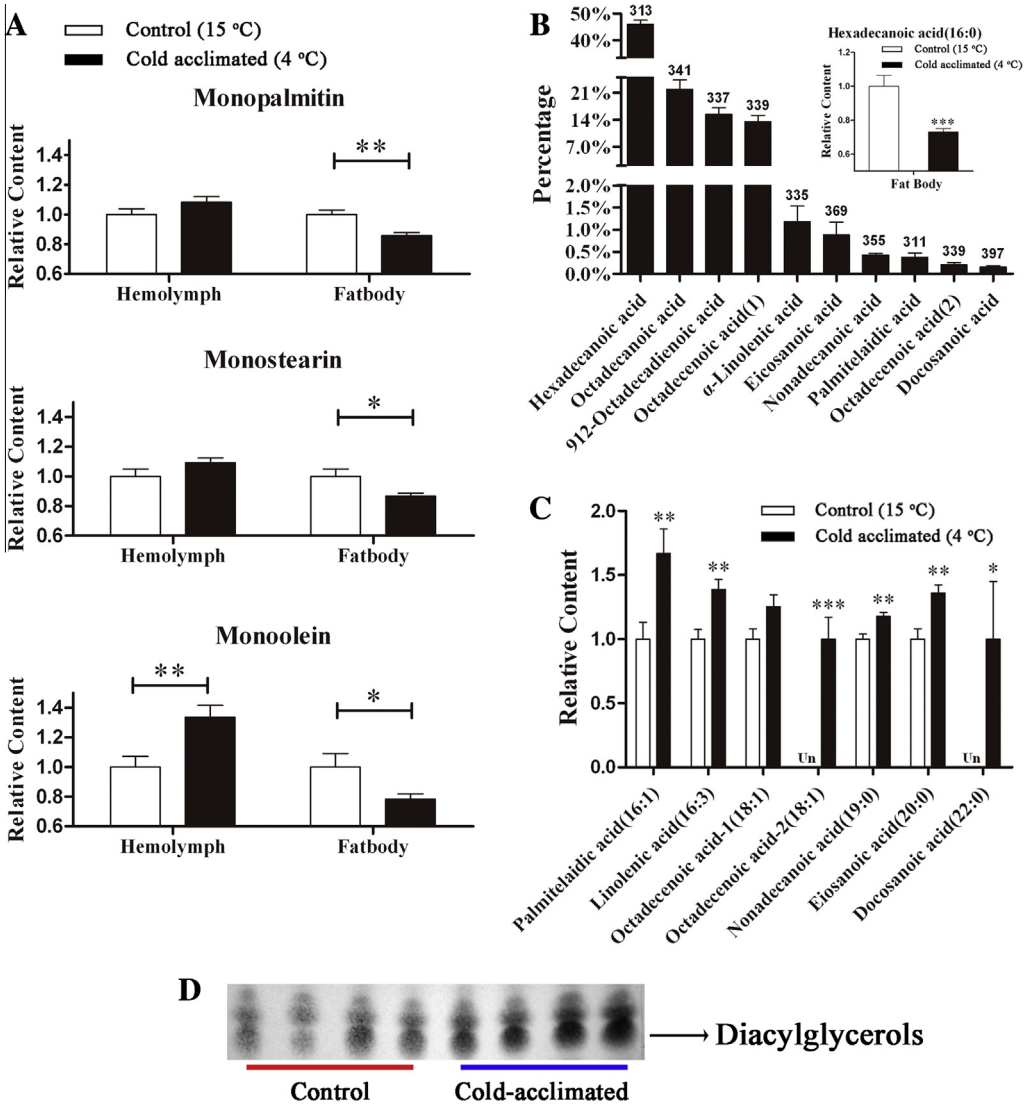

Fig. 4. Mobilization of lipid intermediates in *H. xiaojinensis* larvae. (A). The relative content of monoacylglycerol in the hemolymph and fat body. (B). The composition of free fatty acids in the fat body of *H. xiaojinensis* larvae calculated by respective characteristic ion peak (above the error bars) and presented as percentages. The subgraph shows variation in hexadecanoic acid in fat body. (C). Variation in free fatty acids in hemolymph. (D). Variation in total DAG in hemolymph after thermal acclimation (by TLC). Each column represents the mean ± SE of 12 samples. ***: $p < 0.001$, **: $p < 0.01$, *: $p < 0.05$.

acid and sedoheptulose-7-p) decreased in content (Fig. 3C). However, the transcriptions of phosphofructokinase, glyceraldehyde phosphate dehydrogenase and pyruvate kinase were up-regulated (Fig. 3B). Though glyceraldehyde phosphate dehydrogenase is shared by glycolysis and gluconeogenesis, phosphofructokinase and pyruvate kinase catalyze two irreversible reactions which are specialized in glycolysis. Increased transcription of enzymes in the glycolytic pathway was verified by the high levels of glycerate-3-p and pyruvate (two glycolytic intermediates) relative to that of upstream hexoses and hexose phosphates in cold-acclimated larvae (Fig. 3A). Real-time PCR also indicated that pyruvate dehydrogenase kinase (PDK) was sharply downregulated at the transcriptional level (Fig. 3B). PDK inactivates pyruvate dehydrogenase (PDH), the enzyme controlling pyruvate entering the TCA cycle for aerobic metabolism (Behal et al., 1993; Patel and Korotchkina, 2001). Hence, an up-regulation of activity of PDH would be expected from the down-regulation of PDK.

The pentose phosphate pathway provides NADPH and carbon skeletons for biosynthesis of functional metabolites or structural units of biomacromolecules (Vander Heiden et al., 2009). It also plays a role in cold adaptation of ectotherms by providing NADPH for synthesis of cryprotectants (mainly glycerol and sorbitol) (Holden and Storey, 1994; Storey et al., 1981, 1991) and defence of oxidative damage (Ramnanan and Storey, 2006). However, biosyntheses of cellular components, especially biomacromolecules, are mostly energy and resource intensive processes (Hochachka et al., 1996). In cold-acclimated *H. xiaojinensis* larvae, lower concentrations of glucose, fructose, glucose-6-p and fructose-6-p at 4 °C, whether a result of passive influence or active regulation, may be important in limiting the intensity of the pentose phosphate pathway and therefore reduce the energy budget. Such a deduction is supported by the tight linear correlation between fructose-6-p/glucose-6-p and sedoheptulose-7-p (Fig. 3D), reduced content of glycerol (Fig. S2-A) and increased correlation between glycerol and sugar phosphates (Fig. S2-B) in the cold group. On the other hand, the glycolytic pathway and downstream aerobic metabolism were exclusively compensated by improving the transcription of related enzymes, suggesting that energy metabolism gained priority in utilization of fructose-6-p/glucose-6-p. During diapause of some insects, the expression of

Table 1
List of detected fatty acids in fat body. Contents presented as mean ± SE as percentages. Bold font emphasizes significant variation between groups (q-value < 0.05, FDR adjusted p-value from T-test). SFA = saturated fatty acids, MUFA = monounsaturated fatty acids, PUFA = polyunsaturated fatty acids.

	C:D	Cold-acclimated (n = 3)	Control (n = 4)	p-Value	q-Value
Pentadecanoic acid	15:0	0.039 ± 0.004	0.032 ± 0.001	0.168	0.304
Hexadecanoic acid	16:0	32.406 ± 0.554	31.892 ± 1.038	0.711	0.468
Hexadecenoic acid	16:1	0.516 ± 0.069	0.521 ± 0.048	0.954	0.583
Octadecanoic acid	18:0	1.634 ± 0.147	1.479 ± 0.149	0.502	0.439
Octadecenoic acid	18:1	52.446 ± 0.474	54.103 ± 0.115	0.011	**0.047**
Octadecadienoic acid	18:2	11.386 ± 1.022	10.325 ± 1.079	0.521	0.440
Octadecatrienoic acid	18:3	1.123 ± 0.053	1.292 ± 0.083	0.178	0.304
Eicosanoic acid	20:0	0.118 ± 0.009	0.107 ± 0.014	0.585	0.440
Eicosenoic acid	20:1	0.072 ± 0.008	0.084 ± 0.001	0.150	0.304
Eicosadienoic acid	20:2	0.058 ± 0.011	0.048 ± 0.009	0.502	0.440
Docosanoic acid	22:0	0.081 ± 0.017	0.055 ± 0.011	0.230	0.327
SFA	\	34.277 ± 0.562	33.564 ± 1.056	0.616	0.440
MUFA	\	53.035 ± 0.462	54.708 ± 0.146	0.011	**0.047**
PUFA	\	12.568 ± 0.981	11.666 ± 1.154	0.596	0.440

genes in glycolysis may also be up-regulated to maintain some extent of ATP production (Hahn and Denlinger, 2011), however, the downstream aerobic process was not likely encouraged. In torpid animals, extra expression of PDK is induced to depress the activity of PDH, and finally reduces the overall activity of aerobic metabolism (Andrews et al., 1998; Buck et al., 2002).

3.2.2. Compensatory mobilization of lipids

Three monoacylglycerols (MAGs) were identified in hemolymph and fat body samples of *H. xiaojinensis* larvae: monopalmitin, monostearin and monoolein. In cold-acclimated larvae, MAGs content showed increasing and decreasing trends in hemolymph and fat body, respectively (Fig. 4A). It seems that cold acclimation promoted the transport of MAGs from the fat body to hemolymph. Among the three MAGs, monoolein was the only one containing an unsaturated fatty acid, with the most significant variation in content. Metabolomics also identified 10 free fatty acids (FFAs) in *H. xiaojinensis* larvae (Fig. 4B). Hexadecanoic acid was the most abundant one in the fat body of *H. xiaojinensis* larvae (Fig. 4B), and it was also the only one that changed in the fat body after cold acclimation, with a reduction of 23% in content ($p < 0.001$, Fig. 4B). Unlike MAGs, decreasing hexadecanoic acid in the fat body did not result in a corresponding increase in hemolymph. Instead, the contents of most unsaturated and long chain FFAs in the hemolymph of cold-acclimated larvae were maintained at higher levels than that of control larvae (Fig. 4C). The results from TLC suggest that cold-acclimated larvae contained higher DAG content in their hemolymph (Fig. 4D).

Before lipids are utilized for energy metabolism in insects, triacylglycerols (TAGs) are first broken down in the fat body, the major site for the storage of lipids in insects, and intermediates are packed and transported into the circulatory system for further degradation in various tissues (Arrese et al., 2001). Cold-acclimated *H. xiaojinensis* larvae increased total DAG, MAGs and FFAs in their hemolymph and decreased MAGs in their fat body. The opposite trend in tissues indicates that the mobilization and utilization of lipids was promoted. During the mobilization of triacylglycerides, unsaturated ones are always preferentially mobilized across insects, birds and mammals (reviewed by Hahn and Denlinger, 2011) and this is why monoolein and unsaturated fatty acids underwent greater increases in hemolymph than other MAGs and FFAs in our data. Hexadecanoic acid is the first fatty acid produced during fatty acid synthesis and the precursor to longer and unsaturated fatty acids (Dijkstra et al., 2008). Its reduction in the fat body may be the result of reduced de novo synthesis of fatty acids or enhanced transition to other fatty acids.

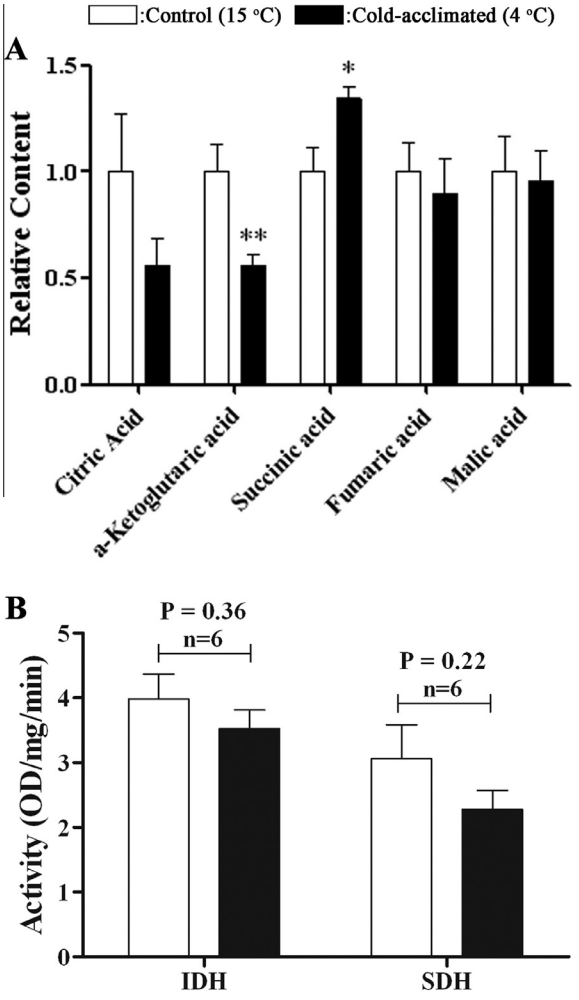

Fig. 5. Compensation strategies in the TCA cycle. (A). Variation in metabolites in the TCA cycle (n = 12, mean ± SE). (B). Activity of enzymes for IDH and SDH (n = 6, mean ± SE). **: $p < 0.01$, *: $p < 0.05$.

We determined the influence of cold acclimation on the composition of total fatty acids in the fat body. A total of 11 fatty acids were detected in our study (Table 1). Among them, octadecenoic acid (18:1) was the most abundant, occupying more than half of total content in control and cold-acclimated groups. Considering that the proportion of TAGs is much larger than that of other lipid

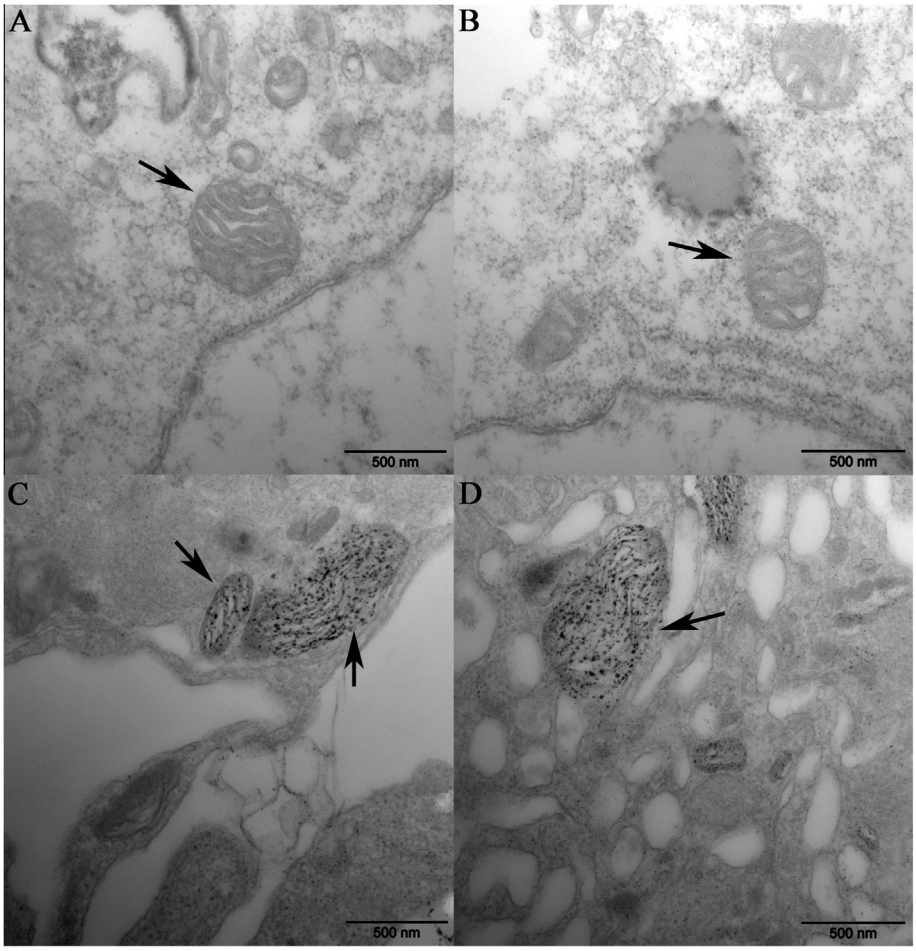

Fig. 6. Transmission electron micrographs of mitochondria in midguts. (A) and (B), mitochondria in midgut cells of the control group. (C) and (D), mitochondria in midgut cells of the cold-treated group. Arrows indicate mitochondria.

classes (phospholipid, MDGs, MAGs and FFAs) in the fat body of insects with normal feeding activity (Buckner and Hagen, 2003; Martin, 1969; Pennington et al., 1996; Uner, 1988), octadecenoic acid was likely the major component of lipid reserve (TAGs) in *H. xiaojinensis* larvae. Cold acclimation resulted in a reduction in the proportion of octadecenoic acid without corresponding increases in the proportions of other fatty acids. Such a phenomenon likely resulted from enhanced mobilization of TAGs at lower temperatures and is consistent with the increased concentration of monoolein (containing an octadecenoic acid) and free octadecenoic acid in the hemolymph of cold-acclimated larvae (Fig. 4A and C).

The improved mobilization of lipids suggests an increased role of lipids in energy metabolism in cold-acclimated *H. xiaojinensis* larvae, in consistent with their RQ values at 4 °C. Such compensation strategies to energy metabolism have been observed in cold-acclimated temperate-zone fish. In these cases, the capacities of oxidation of lipids as well as the relative utilization of lipids were improved to replace the major role of carbohydrates in energy metabolism (Guderley and St-Pierre, 2002; Moerland and Sidell, 1981; Rodnick and Sidell, 1994). Lipids are also a major energy reserve in diapause (a metabolic suppression state) in insects (Hahn and Denlinger, 2011). Rider et al. (2011) reported that lipogenesis was suppressed, while lipolysis was promoted, in diapausing *Epiblema scudderiana* larvae. Therefore, promoting the mobilization of lipids seems to be shared by thermal compensation and metabolic suppression strategies, at least in some cases. For *H. xiaojinensis* larvae, a RQ of 0.69 at 4 °C (Fig. 1) implies that the lipids metabolism pathway is less sensitive to variation in temperature than glycometabolism, so improved lipids mobilization should be more effective and constitute an important compensation strategy in upstream processes of energy production.

3.3. Regulation of aerobic metabolism

3.3.1. TCA cycle compensation

According to variation in metabolites in the TCA cycle in fat bodies (Fig. 5A), metabolites anterior to α-ketoglutarate dehydrogenase (α-KDGH) were down regulated, while those posterior to it were unchanged or higher in cold-acclimated larvae. The pump-like phenomenon between α-ketoglutarate and succinate suggests that flux throughout the TCA cycle was compensated by reinforcing the activity of α-KDGH. The quantitative variation of metabolites also indicates that IDH and SDH are not potential compensation targets (Fig. 5A) and this concurs with the determination of their enzymatic activity (Fig. 5B).

The TCA cycle is the common pathway for complete oxidation of carbohydrates, lipids and amino acids, and when suppressed, results in an overall reduction in the intensity of aerobic metabolism. Enzymes in the TCA cycle are crucial regulation targets in the thermal compensation strategies of ectotherms. For example, the activity of IDH in lugworms living in the subpolar zone (average annual temperature, 4 °C) is higher than those living in boreal zones (average annual temperature, 10 °C) (Sommer and Pörtner, 2002). In temperate-zone fish, the maximum activity of citrate synthase

(CS) is improved by cold acclimation (Fudge et al., 1997; Kleckner and Sidell, 1985; St-pierre et al., 1998). These enzymes are also regulation targets in metabolic suppression of insects, but in an opposite manner. In the dormancy of *E. scudderiana* and *Eurosta solidaginis*, the activity of CS and IDH decreased by 50% (Joanisse and Storey, 1994). In our study, it is likely that the activity of α-KDGH was the compensation target of flux throughout the TCA cycle. Although CS, α-KDGH, IDH and SDH are all crucial regulation targets of the TCA cycle (Nunes-Nesi et al., 2013), the activity of α-KDGH is the lowest among enzymes in the TCA cycle (Hansford, 1980; Lai et al., 1977). It makes sense that the activity of α-KDGH is the primary valve in limiting flux throughout the TCA cycle under cold stress. From another perspective, TCA cycle is the major pathway for transforming the organic carbon of metabolic substrates into CO_2, with two reactions catalyzed by IDH and α-KDGH. The compensatory effect on the TCA cycle (or more exactly, on α-KDGH) directly explains the increased metabolic rate observed here (presented as production rate of CO_2).

3.3.2. Mitochondrial ultrastructure

Compensation effects were also observed at the subcellular level. Mitochondria in midgut cells of cold-acclimated larvae possessed a higher cristae density than control larvae, and the cristae diameter and internal compartment between cristaes were also smaller (Fig. 6). Increasing mitochondrial volume density or cristae density can effectively enlarge the total surface area of the inner mitochondrial membrane, the site for oxidative phosphorylation, and improve the efficiency of ATP production. It is a universal compensation strategy in the muscle fibers of cold-acclimated (1–5 °C) temperate-zone fish (Guderley, 2004). In hypometabolic states, however, the capacity of mitochondria is down-regulated to depress the consumption of metabolic reserves. Insects in dormancy always have decreased mitochondrial number, and reduced RNA and DNA levels (Kukal et al., 1989; Lefebvre and Fourche, 1985; Levin et al., 2003; McMullen and Storey, 2008). Therefore, though insects in metabolic compensation and suppression might share some common adjustments on glycolysis and mobilization of lipids, their aerobic metabolic processes are regulated in an opposite manner. In both cold adaptive strategies, metabolism is likely re-sculpted to shift to a more catabolic poise, suggesting that maintaining energy metabolism is crucial for survival under cold stress. However, insects in metabolic suppression rely on limited resource reserves to sustain long-term supply of energy, which determines their hypometabolic manner, while thermal compensation amis to maintain the capacity of environmental exploitation. In our study, improved mitochondrial cristae density in the midgut emphasizes the importance of sustaining the capacity for digestion and absorption during cold adaptation. Similar to the compensation effect on locomotivity in temperate-zone fish (Guderley, 2004), higher energy production in the midgut can also improve the capacity of environmental exploitation of organisms and in turn fuel overall energy metabolism (Cossins and Bowler, 1987).

4. Conclusion

Ghost moths are a good thermal compensation model for investigating compensation mechanisms in insects. Our research on *H. xiaojinensis* indicates that the energy metabolism system of ghost moths is as sensitive to the cold as in other insects, and that glycometabolism is more susceptible to variation in temperature than lipid metabolism. Cold acclimation induced integrated compensation strategies for energy metabolism and spanned the whole process of catabolism, from promoting complete oxidation of carbohydrates, improving lipids mobilization, encouraging flux throughout the TCA cycle and remodeling mitochondrial ultrastructure. These strategies improved the metabolic rate under low temperatures and explain how ghost moths sustain feeding activity, locomotion and growth at low temperatures. We also found that major differences between thermal compensation and metabolic suppression in insects is their opposite variation in aerobic metabolic activity. Further, thermal compensation strategies in ghost moths are similar to those of temperate-zone fishes, suggesting conserved regulation mechanisms amongst ectotherms. However, the specific mechanism may be species variable, like the different key regulation sites in TCA cycle in ghost moth, lugworm and temperate-zone fish.

Acknowledgements

We thank Dr. Xiongzhao He for helpful comments and suggestions on writing of the manuscript. We also thank anonymous reviewers for their constructive criticisms of this manuscript. This research was supported by the National Science Foundation of China (31272366) and State Key Laboratory of Integrated Management of Pest Insects and Rodents (Chinese IPM 1414).

Appendix A. Supplementary data

Supplementary data associated with this article can be found, in the online version, at http://dx.doi.org/10.1016/j.jinsphys.2015.11.008.

References

Addo-Bediako, A., Chown, S.L., Gaston, K.J., 2002. Metabolic cold adaptation in insects: a large-scale perspective. Funct. Ecol. 16, 332–338.
Andrews, M.T., Squire, T.L., Bowen, C.M., Rollins, M.B., 1998. Low-temperature carbon utilization is regulated by novel gene activity in the heart of a hibernating animal. Proc. Natl. Acad. Sci. 95, 8392–8397.
Arrese, E.L., Canavoso, L.E., Jouni, Z.E., Pennington, J.E., Tsuchida, K., Wells, M.A., 2001. Lipid storage and mobilization in insects: current status and future directions. Insect Biochem. Mol. Biol. 31, 7–17.
Bao, F.Y., Zhang, M., 2013. Determination of triglyceride content in oils and fats by thin layer chromatography. Food Sci. 34, 125–128.
Behal, R.H., Buxton, D.B., Robertson, J.G., Olson, M.S., 1993. Regulation of the pyruvate dehydrogenase multienzyme complex. Annu. Rev. Nutr. 13, 497–520.
Behrends, V., Tredwell, G.D., Bundy, J.G., 2011. A software complement to AMDIS for processing GC–MS metabolomic data. Anal. Biochem. 415, 206–208.
Bligh, E.G., Dyer, W.J., 1959. A rapid method of total lipid extraction and purification. Can. J. Biochem. Physiol. 37, 911–917.
Block, W., 1990. Cold tolerance of insects and other arthropods. Philos. Trans. R. Soc. B 326, 613–633.
Buck, M.J., Squire, T.L., Andrews, M.T., 2002. Coordinate expression of the PDK4 gene: a means of regulating fuel selection in a hibernating mammal. Physiol. Genomics 8, 5–13.
Buckner, J.S., Hagen, M.M., 2003. Triacylglycerol and phospholipid fatty acids of the silverleaf whitefly: composition and biosynthesis. Arch. Insect Biochem. Physiol. 53, 66–79.
Bundy, J.G., Davey, M.P., Viant, M.R., 2008. Environmental metabolomics: a critical review and future perspectives. Metabolomics 5, 3–21.
Chen, S.J., Yin, D.H., Zhong, G.Y., Huang, T.F., 2002. Study on the biology of adults parasite of *Cordyceps sinensis*, *Hepialusbrruensis*. China J. Chin. Mater. Med. 27, 893–895.
Cossins, A.R., Bowler, K., 1987. Temperature Biology of Animals. Chapman and Hall, New York.
Dijkstra, A.J., Hamilton, R.J., Hamm, W., 2008. Fatty Acid Biosynthesis. Wiley-Blackwell, Oxford.
Fudge, D.S., Stevens, E.D., Ballantyne, J.S., 1997. Enzyme adaptation along a heterothermic tissue: the visceral retia mirabilia of the bluefin tuna. Am. J. Physiol. 272, R1834–R1840.
Glanville, E.J., Seebacher, F., 2006. Compensation for environmental change by complementary shifts of thermal sensitivity and thermoregulatory behaviour in an ectotherm. J. Exp. Biol. 209, 4869–4877.
Guderley, H., 2004. Metabolic responses to low temperature in fish muscle. Biol. Rev. 79, 409–427.
Guderley, H., St-Pierre, J., 2002. Going with the flow or life in the fast lane: contrasting mitochondrial responses to thermal change. J. Exp. Biol. 205, 2237–2249.
Guo, X., Liu, B., Ma, S.B., Gui, M.Y., 2008. The ecological environmental investigation and biological characteristic analysis of *Codyceps sinensis* in Yunnan province. Edible Fungi China 27, 8–11.

Hahn, D.A., Denlinger, D.L., 2011. Energetics of insect diapause. Annu. Rev. Entomol. 56, 103–121.
Hansford, R.G., 1980. Control of mitochondrial substrate oxidation. Curr. Top. Bioenerg. 10, 217–278.
Hochachka, P.W., Buck, L.T., Doll, C.J., Land, S.C., 1996. Unifying theory of hypoxia tolerance: molecular/metabolic defense and rescue mechanisms for surviving oxygen lack. Proc. Natl. Acad. Sci. 93, 9493–9498.
Holden, C.P., Storey, K.B., 1994. 6-phosphogluconate dehydrogenase from a freeze tolerant insect: control of the hexose monophosphate shunt and NADPH production during cryprotectant synthesis. Insect Biochem. Mol. Biol. 24, 167–173.
Horwath, K.L., Duman, J.G., 1983. Preparatory adaptations for winter survival in the cold hardy beetles, *Dendroides canadensis* and *Dendroides concolor*. J. Comp. Physiol. 151, 225–232.
Huey, R.B., Pascual, M., 2009. Partial thermoregulatory compensation by a rapidly evolving invasive species along a latitudinal cline. Ecology 90, 1715–1720.
Jin, Y.X., Xu, B., Yang, X.C., Qin, Z.H., Gao, M.F., Lu, H.Y., Zhu, L.B., 2010. The spatial distribution of *Cordyceps sinensis* in Nakchu Prefecture of Tibetan Plateau. Acta Ecol. Sin. 30, 1532–1538.
Joanisse, D.R., Storey, K.B., 1994. Mitochondrial enzymes during overwintering in two species of cold-hardy gall insects. Insect Biochem. Mol. Biol. 24, 145–150.
Kang, J.X., Wang, J., 2005. A simplified method for analysis of polyunsaturated fatty acids. BMC Biochem. 6, 5.
Kleckner, N., Sidell, B.D., 1985. Comparisons of maximal activities of enzymes from tissues of thermally-acclimated and naturally-acclimatized chain pickerel (*Esox niger*). Physiol. Zool. 58, 18–28.
Kukal, O., Duman, J., Serianni, A., 1989. Cold-induced mitochondrial degradation and cryoprotectant synthesis in freeze-tolerant arctic caterpillars. J. Comp. Physiol. B 158, 661–671.
Lachenicht, M.W., Clusella-Trullas, S., Boardman, L., Le Roux, C., Terblanche, J.S., 2010. Effects of acclimation temperature on thermal tolerance, locomotion performance and respiratory metabolism in *Acheta domesticus* L. (Orthoptera: Gryllidae). J. Insect Physiol. 56, 822–830.
Lai, J.C., Walsh, J.M., Dennis, S.C., Clark, J.B., 1977. Synaptic and non-synaptic mitochondria from rat brain: isolation and characterization. J. Neurochem. 28, 625–631.
Layne-Jr, J.R., Edgar, C.L., Medwith, R.E., 1999. Cold hardiness of the woolly bear caterpillar (*Pyrrharctia isabella* Lepidoptera Arctiidae). Am. Midl. Nat. 141, 293–304.
Lee Jr., R.E., 2010. A Primer on Insect Cold-Tolerance. Cambridge University Press, Cambridge.
Lefebvre, F., Fourche, J., 1985. Mitochondrial aspects of cold acclimation in *Pieris brassicae* (Lepidoptera) during diapause and post-diapause imaginal development. J. Therm. Biol 10, 29–33.
Levin, D.B., Danks, H.V., Barber, S.A., 2003. Variations in mitochondrial DNA and gene transcription in freezing-tolerant larvae of *Eurosta solidaginis* (Diptera: Tephritidae) and *Gynaephora groenlandica* (Lepidoptera: Lymantriidae). Insect Mol. Biol. 12, 281–289.
Liu, F., Wu, X.L., Chen, S.J., Yin, D.H., Zeng, W., Zhong, G.Y., 2007. Advances in studies on artificial culture of *Cordyceps sinensis*. Chin. Tradit. Herb. Drugs 38, 302–305.
Martin, J.S., 1969. Lipid composition of fat body and its contribution to the maturing oojcytes in Pyrrhocorisapterus. J. Insect Physiol. 15, 1025–1045.
McMullen, D.C., Storey, K.B., 2008. Mitochondria of cold hardy insects: Responses to cold and hypoxia assessed at enzymatic, mRNA and DNA levels. Insect Biochem. Mol. Biol. 38, 367–373.
Michaud, M.R., Benoit, J.B., Lopez-Martinez, G., Elnitsky, M.A., Lee Jr., R.E., Denlinger, D.L., 2008. Metabolomics reveals unique and shared metabolic changes in response to heat shock, freezing and desiccation in the Antarctic midge, *Belgica antarctica*. J. Insect Physiol. 54, 645–655.
Moerland, T.S., Sidell, B.D., 1981. Characterization of metabolic carbon flow in hepatocytes isolated from thermally acclimated killifish *Fundulus heteroclitus*. Physiol. Zool. 54, 379–389.
Mustonen, A.M., Kakela, R., Nieminen, P., 2007. Different fatty acid composition in central and peripheral adipose tissues of the American mink (*Mustela vison*). Comp. Biochem. Physiol. A 147, 903–910.
Nicholson, J.K., Lindon, J.C., 2008. Systems biology: metabonomics. Nature 455, 1054–1056.
Nunes-Nesi, A., Araújo, W.L., Obata, T., Fernie, A.R., 2013. Regulation of the mitochondrial tricarboxylic acid cycle. Curr. Opin. Plant Biol. 16, 335–343.
Oda, Y., Iwami, M., Osanai, M., Sakurai, S., 1997. Dynamics of haemolymph sorbitol-6-phosphate and its control by ecdysteroid in the larvae of the silkworm, *Bombyxmori*. Insect Biochem. Mol. Biol. 27, 461–468.
Pasikanti, K.K., Ho, P.C., Chan, E.C., 2008. Gas chromatography/mass spectrometry in metabolic profiling of biological fluids. J. Chromatogr. B 871, 202–211.
Patel, M.S., Korotchkina, L.G., 2001. Regulation of mammalian pyruvate dehydrogenase complex by phosphorylation: complexity of multiple phosphorylation sites and kinases. Exp. Mol. Med. 33, 191–197.
Pennington, J.E., Nussenzveig, R.H., Heusden, M.C.V., 1996. Lipid transfer from insect fat body to lipophorin: comparison between a mosquito triacylglycerol-rich lipophorin and a sphinx moth diacylglycerol-rich lipophorin. J. Lipid Res. 37, 1144–1152.
R Core Team, 2014. R: A Language and Environment for Statistical Computing. R Foundation for Statistical Computing, Vienna, Austria.
Ramnanan, C.J., Storey, K.B., 2006. Glucose-6-phosphate dehydrogenase regulation during hypometabolism. Biochem. Biophys. Res. Commun. 339, 7–16.
Rider, M.H., Hussain, N., Dilworth, S.M., Storey, J.M., Storey, K.B., 2011. AMP-activated protein kinase and metabolic regulation in cold-hardy insects. J. Insect Physiol. 57, 1453–1462.
Rodnick, K.J., Sidell, B.D., 1994. Cold acclimation increases carnitine palmitoyltransferase I activity in oxidative muscle of striped bass. Am. J. Physiol. 266 (2), R405–R412.
Schiesari, L., O'Connor, M.B., 2013. Chapter eight – diapause: delaying the developmental clock in response to a changing environment. In: Ann, E.R., Michael, B.O.C. (Eds.), Current Topics in Developmental Biology. Academic Press, pp. 213–246.
Sommer, A., Pörtner, H.-O., 2002. Metabolic cold adaptation in the lugworm *Arenicola marina* (L.): comparison of a White Sea and a North Sea population. Mar. Ecol. Prog. Ser. 240, 171–182.
Storey, K.B., Baust, J.G., Storey, J.M., 1981. Intermediary metabolism during low temperature acclimation in the overwintering gall fly larva, *Eurosta solidaginis*. J. Comp. Physiol. 144, 183–190.
Storey, K.B., Keefe, D., Kourtz, L., Storey, J.M., 1991. Glucose-6-phosphate dehydrogenase in cold hardy insects: kinetic properties, freezing stabilization, and control of hexose monophosphate shunt activity. Insect Biochem. 21, 157–164.
Storey, K.B., Storey, J.M., 2004. Metabolic rate depression in animals: transcriptional and translational controls. Biol. Rev. 79, 207–233.
St-pierre, J., Charest, P.M., Guderley, H., 1998. Relative contribution of quantitative and qualitative changes in mitochondria to metabolic compensation during seasonal acclimatisation of rainbow trout, *Oncorhynchus mykiss*. J. Exp. Biol. 201, 2961–2970.
Sumner, L.W., Amberg, A., Barrett, D., Beale, M.H., Beger, R., Daykin, C.A., Fan, T.W., Fiehn, O., Goodacre, R., Griffin, J.L., Hankemeier, T., Hardy, N., Harnly, J., Higashi, R., Kopka, J., Lane, A.N., Lindon, J.C., Marriott, P., Nicholls, A.W., Reily, M.D., Thaden, J.J., Viant, M.R., 2007. Proposed minimum reporting standards for chemical analysis Chemical Analysis Working Group (CAWG) Metabolomics Standards Initiative (MSI). Metabolomics 3, 211–221.
Sung, G.H., Hywel-Jones, N.L., Sung, J.M., Luangsa-Ard, J.J., Shrestha, B., Spatafora, J. W., 2007. Phylogenetic classification of Cordyceps and the clavicipitaceous fungi. Stud. Mycol. 57, 5–59.
Tauber, M.J., Tauber, C.A., Masaki, S., 1986. Seasonal Adaptations of Insects. Oxford University Press, New York.
Tschischka, K., Abele, D., Portner, H.O., 2000. Mitochondrial oxyconformity and cold adaptation in the polychaete Nereispelagica and the bivalve *Arctica islandica* from the Baltic and White Seas. J. Exp. Biol. 203, 3355–3368.
Tu, Y.Q., Zhang, D.L., Zeng, W., Chen, S.J., 2011. Study on biological characteristic of *Hepialus xiaojinensis* in Sichuan. Chin. J. Appl. Entomol. 48, 990–996.
Uner, N., 1988. Lipid composition of the fat body, haemolymph and muscle in Tenebriomolitor L. (Coleoptera: Tenebrionidae) larvae. Commun. Fac. Sci. Univ. Ank. Ser. C 6, 147–157.
Vander Heiden, M.G., Cantley, L.C., Thompson, C.B., 2009. Understanding the Warburg effect the metabolic requirements of cell proliferation. Science 324, 1029–1033.
Vinogradova, E., 2007. Diapause in aquatic insects, with emphasis on mosquitoes. In: Alekseev, V., de Stasio, B., Gilbert, J. (Eds.), Diapause in Aquatic Invertebrates Theory and Human Use. Springer, Netherlands, pp. 83–113.
Wang, H.S., Zeng, H., Xu, H.F., 2006. Study on change regulation of environment factors at *Cordyceps sinensis* growth area. Chin. Qinghai J. Anim. Vet. Sci. 36, 9–10.
Wickham, H., 2009. Ggplot2: Elegant Graphics for Data Analysis. Springer, New York.
Wiegmann, B.M., Regier, J.C., Mitter, C., 2002. Combined molecular and morphological evidence on the phylogeny of the earliest lepidopteran lineages. Zool. Scr. 31, 67–81.
Wishart, D.S., 2007. Current progress in computational metabolomics. Brief. Bioinf. 8, 279–293.
Zhu, Y.J., Duan, S.Q., Ouzhu, L.J., 2009. Advances in the study of *Cordyceps sinensis*. J. CUN (Nat. Sci. Ed.) 18, 27–33.